PCCP

PAPER

View Article Online
View Journal | View Issue

Cite this: *Phys. Chem. Chem. Phys.*, 2015, **17**, 28844

Photoswitching the mechanical properties in Langmuir layers of semifluorinated alkyl-azobenzenes at the air–water interface†

Antigoni Theodoratou,[ab] Ulrich Jonas,*[ac] Benoit Loppinet,[a] Thomas Geue,[d] René Stangenberg,[e] Dan Li,[e] Rüdiger Berger[e] and Dimitris Vlassopoulos[ab]

Received 20th July 2015,
Accepted 21st September 2015

DOI: 10.1039/c5cp04242a

www.rsc.org/pccp

Semifluorinated alkyl-azobenzene derivatives (SFAB) can form stable Langmuir layers at the air–water interface. These systems combine the amphiphobic character of semifluorinated alkyl units as structure-directing motifs with photochromic behavior based on the well-known reversible *cis–trans* isomerization upon irradiation with UV and visible light. Herein, we report our investigations of the structural and dynamic tunability of these SFAB layers at the air–water interface in response to an external light stimulus. The monolayer structures and properties of [4-(heptadecafluorooctyl)phenyl](4-octylphenyl)diazene (F8-azo-H8) and bis(4-octylphenyl)diazene (H8-azo-H8) were studied by neutron reflectivity, surface pressure–area isotherms with compression–expansion cycles, and interfacial rheology. We find that UV irradiation reversibly influences the packing behavior of the azobenzene molecules and interpret this as a transition from organized layer structures with the main axis of the molecule vertically oriented in the *trans* form to random packing of the *cis* isomer. Interestingly, this *trans–cis* isomerization leads to an increase in surface pressure, which is accompanied by a decrease in viscoelastic moduli. These results suggest ways of tailoring the properties of responsive fluid interfaces.

I. Introduction

The term ''reconfigurable'' or ''programmable'' soft matter represents an emerging concept in science and technology, wherein the chemical, physical and functional properties of materials can be switched between well-defined states by external stimulation, for example by irradiation with light.[1] Manifold examples are found in nature, such as the phototaxis of plants (like the head of a sunflower following the sun), and at present the challenge exists in research to harness such powerful behaviour in artificial matter by merging the specific responsive functionality of molecules with a complex structural hierarchy. One strategy to achieve this goal targets the ability of certain types of compounds to self-assemble into complex superstructures and aims to implement this behaviour with appropriate responsive molecules and polymers.[2] For such systems, the final structure of the assembly depends on the presence or absence of the stimulus. Lower-dimensional systems that are made of such responsive materials, such as 2D layer architectures or interdigitating phases, possess a large interface between the different phases and are of particular interest due to their structural organization, as here the interaction between the stimulus and the responsive material is enhanced compared to the bulk material.

Semifluorinated alkanes (SFAs), which contain fluorinated alkyl chains in addition to hydrogenated alkyl moieties, constitute a specific class of materials that can organize into ordered structures due to the mutual incompatibility of the fluorinated and hydrogenated segments. Based on this structure-guiding motif, they have received attention over recent years, for example, due to their ability to form different mesophases in the bulk form upon a decrease in temperature[3] and stable Langmuir layers at an air–water interface *via* hierarchical self-assembly, despite the hydrophobicity of both fluorinated and alkane moieties.[4] The specific challenge with fluid interfaces coated with SFAs is the manipulation of their properties using external stimuli, particularly light. An appropriate class of materials that respond to irradiation with light is photochromic molecules, with one of the most prominent members of this class being azobenzene compounds.

[a] *Foundation for Research and Technology Hellas (FORTH), Institute of Electronic Structure and Laser, 71110 Heraklion, Greece*
[b] *University of Crete, Department of Materials Science and Technology, 71003 Heraklion, Greece*
[c] *University of Siegen, Macromolecular Chemistry, Department of Chemistry and Biology, 57076 Siegen, Germany. E-mail: jonas@chemie.uni-siegen.de; Tel: +49 271 740 4713*
[d] *Paul Scherrer Institute, Laboratory for Neutron Scattering and Imaging, 5232 Villigen, Switzerland*
[e] *Max Planck Institute for Polymer Research, 55128 Mainz, Germany*
† Electronic supplementary information (ESI) available. See DOI: 10.1039/c5cp04242a

Photosensitive azobenzene derivatives reversibly undergo *cis–trans* isomerization upon irradiation with light, *i.e.*, the formation of the bent *cis* isomer by exposure to short-wavelength UV radiation and reconfiguration into the *trans* isomer under visible light. They can exhibit photoinduced optical anisotropy (becoming dichroic and/or birefringent) and therefore are potential candidates for various electro-optical applications[5–7] such as photosensitive devices,[8] photonics,[9] reversible optical data storage[10] and high-density data storage films.[11] Ikeda *et al.*[12] developed azobenzene liquid crystal (LC) films with a nematic phase of the *trans*-isomers (generated by irradiation with laser light) and no LC phase in the *cis* form. Photosensitive materials in general find applications in pharmacotherapy[13] by the incorporation of photoswitchable groups into the molecular structure of bioactive compounds.

For example, photoinduced material transport in thin films was shown with azobenzene-modified polymers *via* surface plasmon near-field radiation from a nanostructured surface coated with these polymers[14] or *via* far-field irradiation to yield topographic patterns with >100 nm variation in height.[15] Furthermore, the expansion factor of single microgel particles in an aqueous suspension could be reversibly controlled by irradiation with light at different wavelengths upon mixing the microgels with azobenzene surfactants.[16]

Wustneck *et al.*[17] investigated the *cis–trans* photoisomerization of monolayers of an azobenzene-containing trifluoromethoxy-substituted methacrylate copolymer at fluid interfaces using surface pressure–area isotherms with the pendant drop technique. It was found that the minimum area required per repeating unit in the *trans* configuration was smaller than that for the *cis* isomer. Accordingly, the tendency to aggregate was higher in the *trans* configuration at a low surface coverage. The restoration of the *trans* configuration depended on the surface pressure.[11]

Ultrathin films of two novel azobenzene-functionalized 1,3,5-triazine-4,6-dithiols were investigated by Muzikante *et al.*[18] Switching from the *trans*- to the *cis* configuration was observed by measuring the surface potential using the Kelvin probe technique while alternating the irradiation of the self-assembled quasi-monolayer between UV and visible light. In the literature, most systems that have been investigated are self-assembled monolayers (SAMs) of azobenzene-containing alkanethiols.[19,20]

Fuller *et al.*[21] studied the interfacial rheology of photosensitive monolayers using azobenzene-containing fatty acids. It was found that the *trans*-configuration yielded a well-packed film with non-Newtonian behaviour, whereas the *cis* configuration resulted in a structureless Newtonian film that could not be oriented by surface flows. Recently, Monteux *et al.*[22] studied the adsorption dynamics of azobenzene-based charged surfactants between an air–water interface and a subphase and found that the *cis* isomer was adsorbed 10 times faster than the *trans* isomer, whereas on the other hand the *cis* isomer was also desorbed 300 times faster. As a result, the surface was enriched in the *trans* isomer within a few seconds and upon illumination with UV or blue light, part of the *trans* population was converted into the *cis* configuration, leading to a rapid increase in the surface tension. Further studies support the higher surface affinity of *trans* isomers and their ability to stabilize foams.[23] In addition, Shang *et al.*[24] investigated neutral surfactants that contained one azobenzene group in their tail and found changes in surface tension and critical micellar concentration. The dependence on temperature of aggregation and dynamic surface tension in a photoresponsive surfactant system at an air–water interface for *cis* and *trans* isomers was investigated by Cicciarelli *et al.*[25,26]

Regarding the kinetics of *trans–cis* isomerization in azobenzene-containing systems, as studied in Langmuir–Blodgett (LB) films, they were found to be of first-order,[27] whereas in a solid glass, deviations have been reported.[28] Kumar *et al.*[29] studied the kinetics of *trans–cis* photoisomerisation in a Langmuir monolayer composed of mesogenic azobenzene dimers at a water–air interface and also found a deviation from first-order kinetics. This effect was attributed to the simultaneous photoisomerisation of *trans* isomers to form *cis* isomers and reverse thermal isomerization of metastable *cis* isomers to form stable *trans* isomers. Finally, LB films of amphiphilic azobenzene derivatives have been used as motifs for macroscopic reorganization in liquid-crystal thin films.[30]

Therefore, it is evident that fluid interfaces decorated with azobenzene moieties exhibit interesting photoresponsive properties and are promising candidates for electro-optical thin-film applications. However, despite the work done so far, a clear link between the interfacial structure and 2D mechanical properties in such responsive materials is missing. This is especially true for systems with the ability to exhibit different levels of hierarchical self-assembly at interfaces such as semifluorinated alkanes.

In the present study, we addressed the abovementioned challenge by investigating the effects of stimulation by UV on the interfacial properties of a novel azobenzene derivative of a semifluorinated alkane, [4-(heptadecafluorooctyl)phenyl](4-octylphenyl)diazene (in short, F8-azo-H8), and its fully hydrogenated analogue, bis(4-octylphenyl)diazene (abbreviated here as H8-azo-H8), both shown in Fig. 1. The semifluorinated alkylazobenzene (SFAB) derivative F8-azo-H8 combines the structure-guiding motif of mutual incompatibility between fluorinated and hydrogenated alkyl chains with the photochromic property of switching molecular configuration by external stimulation with light. This water-insoluble compound can be spread at an air–water interface as stable Langmuir layers to control the mechanical behaviour of this interface in response to light. For both the azobenzene derivatives, we investigated the interfacial organization by means of neutron reflectivity and surface pressure isotherms in a Langmuir trough, whereas the interfacial viscoelasticity was investigated using a magnetic-rod interfacial stress rheometer (ISR). Changes in these properties were examined systematically in response to irradiation by UV and visible light, which was shown to dramatically influence the interfacial packing of the azobenzene molecules. The obtained data suggest a UV light-induced transition of packing structures with a vertically oriented main axis of the molecules into a featureless amorphous film.

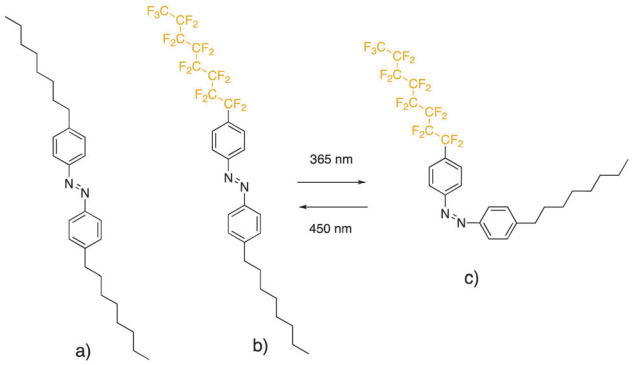

Fig. 1 Chemical structures of (a) bis(4-octylphenyl)diazene (abbreviated as H8-azo-H8), (b) [4-(heptadecafluorooctyl)phenyl](4-octylphenyl)diazene (abbreviated as F8-azo-H8) and (c) the light-induced change in configuration from *trans* to *cis*.

II. Experimental

II.1. Materials

The azobenzene derivative [4-(heptadecafluorooctyl)phenyl](4-octylphenyl)diazene (F8-azo-H8) with one fluorinated and one hydrogenated alkyl chain was synthesized by asymmetric coupling of 1-nitroso-4-octylbenzene (by the oxidation of 4-octylaniline with potassium peroxymonosulfate) with 4-perfluorooctylaniline.[31] Coupling 1-nitroso-4-octylbenzene with 4-octylaniline yielded bis(4-octylphenyl)diazene (H8-azo-H8). The thermodynamic, optical, structural, and dynamic properties of these materials have been reported by Stangenberg *et al.* and the absorption spectra of the *trans* and *cis* configurations are provided in the ESI,† Fig. S12.[32]

II.2. Methods

II.2.1. Surface pressure–area isotherms. Surface pressure (Π)–area (A) isotherms were measured with a commercial Langmuir trough (Minitrough 4, KSV Instruments, Finland) made of hydrophobic Teflon with movable barriers of hydrophilic polyoxymethylene. An amount of 1 mg mL^{-1} of the SFAB compound to be deposited was dissolved in hexane and the solution was spread with a Hamilton glass syringe onto the subphase (consisting of ultrapure water). In the case of F8-azo-H8, 100 μL of the solution was spread in the dark (experimental data labelled "dark") or in the experiments indicated with the label "UV", 50 μL of the SFAB solution was irradiated inside the syringe used for spreading with UV light of 365 nm wavelength before spreading. Photoconversion of the compounds was achieved with a Spectroline UV lamp (365 nm, 6 W tube, irradiated for 10 minutes at a distance of 8 cm, for experimental details see the ESI†). For H8-azo-H8, 200 μL of the solution was spread to obtain the entire isotherm in the dark and 50 μL was spread under UV irradiation (same conditions as irradiation of the syringe). The solvent was allowed to evaporate for at least 10 minutes and subsequently the barriers were compressed/expanded at a speed of 5 to 25 mm min^{-1}. A Wilhelmy plate balance measured the surface pressure, whereas the temperature of the water subphase was maintained at 20 °C in all experiments by means of a water bath circulator. The same set-up was also used for performing compression–expansion cycles in order to examine the mechanical stability of the Langmuir films.

II.2.2. Interfacial rheology. The Langmuir trough was further equipped with an interfacial stress rheometer (ISR), which was originally developed by Brooks *et al.*[33] Two Helmholtz coils in the center of the trough generated a homogeneous magnetic field with the field lines parallel to the air–water interface. A sinusoidal, time-dependent gradient was induced in the magnetic field by modulating the amplitude of the applied voltage in the frequency range from 0.01 to 4 Hz with a frequency generator. A Teflon-coated magnetized rod floating at the air–water interface in a small channel in the centre of the trough served as a rheological probe. The horizontal displacement of the rod due to the field oscillation was monitored as a function of time using a CCD camera (SONY XC-HR50). The rod was positioned at the air–water interface in the channel before spreading the SFAB sample solution. The measurement protocol involved measurements during a dynamic frequency sweep in a linear viscoelastic regime (checked *via* selected dynamic time and strain sweep tests) at various positions of the barriers during compression and expansion cycles, with the light (UV or visible light, respectively) either switched on or off.

II.2.3. Neutron reflectivity. Neutron reflectivity measurements were made at the air–water interface using the Langmuir trough on the AMOR reflectometer of the Swiss Spallation Neutron Source (SINQ) at the Paul Scherrer Institute, Switzerland. Motion of the barriers allowed measurements of reflectivity at different surface pressures, as described in Section II.2.1. The subphase consisted of D_2O. Further details of the instruments and procedures used are described elsewhere.[34,35] Measurements were made at three incident angles (0.6°, 1.4° and 2.4°), which gave a range of momentum transfer Q ($Q = (4\pi \sin\theta)/\lambda$, with λ being the wavelength and θ the angle of incidence) from 0.1 to 1.5 nm^{-1}. The obtained reflectivity data were analysed using the Parratt32 software, version 1.6 (Helmholtz-Zentrum Berlin für Materialien und Energie GmbH, Germany).[36] Taking into account the different possible packing models by varying the structural parameters (number of layers and for each layer, the layer thickness, scattering length density and surface roughness), the scattering density profile is calculated. For each case, three numbers of layers were tested (1 layer, 2 layers and 3 layers). Detailed results for these different fitting models are provided in the ESI.† The scattering length density of each layer was calculated using the NIST's scattering length density calculator,[37] assuming the density of the layer to be the bulk density of each material (for example, the bulk density of the fluorinated alkyl chain was taken to be equal to the density of polytetrafluoroethylene, whereas the hydrogenated alkyl chain was represented by data for polyethylene and the aromatic core was approximated by data for toluene). For each case, the number of layers and the scattering length density were the fixed parameters, whereas the layer thickness and surface roughness were treated as variable parameters for minimization. In the first step the layer thicknesses were fixed at the value expected from the model and in the second step this value was then optimized.

II.2.4. Scanning force microscopy. For scanning force microscopy (SFM), the SFAB films were transferred from the water–air interface to plasma-cleaned silicon wafer substrates (10 min argon plasma). For transfer of the layers, the silicon wafers were located at the bottom of the trough (KSV Minitrough, KSV Instruments Ltd., Finland) with a small tilt angle of around 7° and water was removed by a peristaltic pump (Minipuls 3, Abimed, Gilson Inc., United States) at a speed of approximately 10 mL min^{-1}. The films that were investigated under UV irradiation were initially compressed to a surface pressure of 2 mN m^{-1} and then illuminated with UV light for around 60 min followed by transfer of the film as described above. For the films prepared under visible light, SFAB was spread and compressed to a surface pressure of 2 mN m^{-1} in the dark, then irradiated with UV light for 60 min, kept in the dark for 60 min, and finally white light was switched on. After several hours, the films were transferred onto the silicon wafer.

Directly after the transfer, each sample was analyzed by SFM (MFP-3D, Asylum Research, USA) in the intermittent contact mode. We used silicon cantilevers (Olympus OMCL-AC240TS, nominal tip radius <7 nm, resonance frequency 50–90 kHz, spring constant 0.7–3.8 N m^{-1}). The cantilevers were placed on a glass coverslip and cleaned in argon plasma (PDC-002 plasma cleaner/sterilizer, 200 W, Harrick Scientific Corp., United States) for 30 s at a pressure of approximately 1.6 mbar. The SFM data were flattened and analyzed using the Gwyddion Software (www.gwyddion.net).

III. Results and discussion

III.1. Characterisation of the semifluorinated F8-azo-H8 Langmuir layers

The surface pressure (Π)–molecular area (A) isotherms of F8-azo-H8 measured at the air–water interface are shown in Fig. 2 for different illumination conditions. As a plausibility check, the molecular surface area of the SFAB Langmuir film measured between 40 and 50 mN m^{-1} (*trans* configuration for the "DARK" experiment) was compared with the theoretical surface requirement, which was calculated from the molecular projection area perpendicular to the long axis of the molecule in *trans* configuration, corresponding to the configuration in the "DARK" experiment. The agreement of these two numbers suggests the formation of a true monolayer, with the axis of the alkyl chain being oriented predominantly perpendicular to the air–water interface (and in good agreement with the surface requirement of simple semifluorinated alkanes).[4] After thermal equilibration of the Langmuir film in the absence of light, the azobenzene units of SFAB molecules were predominantly in the *trans* configuration. The *trans–cis* configurational change of the azobenzene units upon irradiation with UV light, which could be reversed by exposure to visible light (above *ca.* 450 nm wavelength), had a direct effect on the surface pressure isotherms, as shown in Fig. 2. During the measurement under UV irradiation (the isotherm labelled "UV"), F8-azo-H8 molecules predominantly existed in the *cis* configuration (about 70% in the photostationary equilibrium) and apparently occupied a molecular area at the onset of the increase in pressure (about 2 mN m^{-1}), which is about three times larger than that in the *trans* configuration (measurements performed in the absence of light, isotherm labelled "DARK"). This is directly linked to molecular reorganization, as will be discussed below based on the neutron reflectivity data. Under visible light, the situation was intermediate, as most molecules reverted from the *cis* to the *trans* form. Moreover, we note that the compression/expansion isotherm was completely reversible in the dark, whereas it exhibited slight hysteresis under irradiation by UV or visible light. Nevertheless, these compression–expansion cycles suggest that even at the highest pressures that were reached (18 mN m^{-1}), there was no evidence of an irreversible collapse of the film or other degradative effects discernible in the isotherms; hence, the applied deformation of the films is fully reversible.

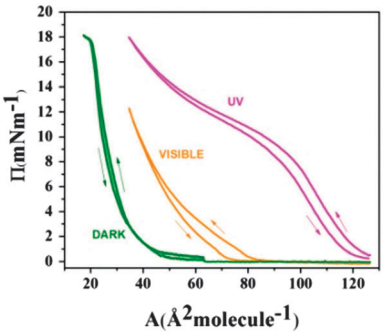

Fig. 2 Surface pressure (Π) *versus* molecular area (A) isotherms of F8-azo-H8 monolayers at an air–water interface at 20 °C under different irradiation conditions: UV light inducing predominantly a *cis* configuration (right curve in purple, labelled "UV"), visible light with *cis* and *trans* configurations (middle curve in orange, "VISIBLE") and in the dark with a *trans* configuration (left curve in green, "DARK"). The arrows indicate the directions of compression and expansion with negligible hysteresis.

The modulation of the internal strain (as expressed by the variation in surface pressure in the isotherms of Fig. 3) of F8-azo-H8 monolayers was examined upon exposure to stimuli from different wavelengths of light. Measurements started at a surface pressure of 2 mN m^{-1} in the dark (corresponding to the onset of the slope in Fig. 2) and after about 1 hour the UV lamp

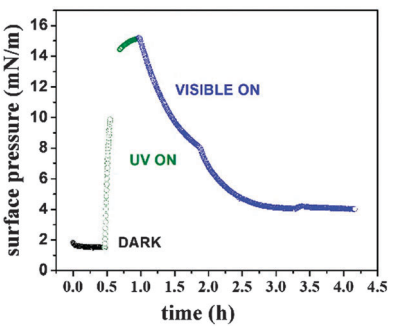

Fig. 3 Variation of the surface pressure over time for a F8-azo-H8 monolayer for different light stimuli (pure water subphase, 20 °C) under dark (green), UV (purple), dark (black) and visible-light (blue) conditions.

was switched on. During this irradiation, the surface pressure increased and reached a maximum value of about 16 mN m^{-1} within about 1 hour. Then, the monolayer was exposed to visible light and the surface pressure dropped to 4 mN m^{-1} after 3 hours.

The responsiveness of the F8-azo-H8 monolayer to conditions of light irradiation was also reflected in the corresponding modulation of its viscoelastic properties. This is demonstrated by the dynamic time sweep measurements in Fig. 4, which depict UV-induced changes in the storage (G') and loss (G'') moduli.

In the course of the experiment, the conditions changed from dark (at a surface pressure of 12 mN m^{-1}) to UV irradiation. This resulted in a change in the surface pressure (increasing to 17 mN m^{-1}), which was apparently caused by a structural reorganization of the F8-azo-H8 film (discussed further below) that led to a decrease in G' and G'' by about one order of magnitude when UV light was switched on. Note that the responses of the moduli were almost instantaneous when changing irradiation levels, whereas for static lighting conditions the moduli were constant. It can be noted that the moduli were very weak (in fact barely resolved) and the response of the F8-azo-H8 monolayers was liquid-like. This is further confirmed by analysis of the apparent Poisson ratio of the films. The compression modulus, $\varepsilon = -A\ \mathrm{d}\pi/\mathrm{d}A$, which was derived from the pressure area-isotherms, was of the order of 10 mN m^{-1}, essentially orders of magnitude higher than the shear modulus (Fig. 4). Hence, the Poisson ratio of the 2D layer was $\nu = \varepsilon - G/\varepsilon + G = 1$, which is the expected value for a liquid interface.[38]

A series of viscoelasticity measurements for different combinations of surface pressures and irradiation conditions (UV *versus* dark) is presented in Fig. 5. As a general trend, we find that the G' modulus was reduced upon UV irradiation (which is consistent with Fig. 4), whereas at the same time the surface pressure increased (which is consistent with Fig. 3). From these results, it can be further concluded that the lower the initial surface pressure in the dark, the larger the jump in surface pressure and the lower the decrease in the modulus when UV light was switched on. These results raise the question of which structural change upon irradiation is related to this shift in surface pressure and moduli. A potential answer may be given by the SFM results presented further below (Fig. 8), which indicate a tendency of the *cis* conformer to form 3D aggregates at a confined surface area (and a consequent increase in surface pressure) under UV irradiation. Thus, we discuss below the structural analysis of the films, which was performed by neutron reflectivity measurements.

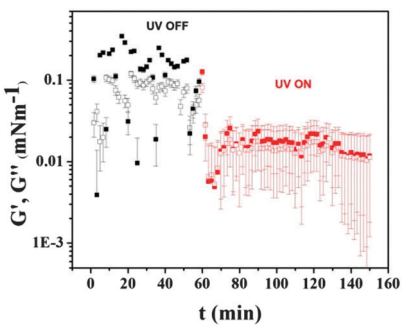

Fig. 4 Dynamic time sweep measurements of storage (G', closed symbols) and loss (G'', open symbols) moduli for a F8-azo-H8 monolayer at an air–water interface at a temperature of 20 °C, frequency of ω = 0.6 rad s^{-1} and strain amplitude of γ_0 = 0.1% using a magnetic-rod interfacial stress rheometer. The measurements started at a surface pressure of 12 mN m^{-1}. Light conditions: UV off (first 60 min), then UV on.

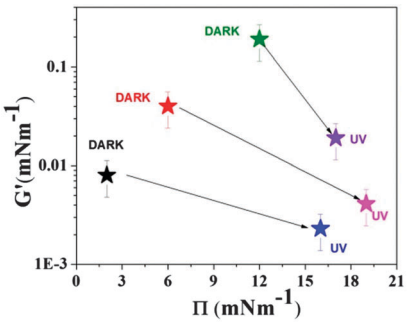

Fig. 5 Storage modulus (G') *versus* surface pressure of the F8-azo-H8 monolayer at the air–water interface showing the decrease by an order of magnitude in the elastic modulus under UV irradiation for three different starting surface pressures (Π): Π = 2 mN m^{-1}, Π = 6 mN m^{-1} and Π = 12 mN m^{-1}.

The results from the neutron reflectivity experiments are presented in Fig. 6, where the scattering curves are shown as normalized intensity *versus* q for the F8-azo-H8 layer in comparison to the bare D_2O subphase in the dark (Fig. 6a) and under UV irradiation (Fig. 6b). In the upper insets of these figures, we show the same data in a more sensitive representation (normalized intensity (NR) × q^4 *versus* q), which allows us to better distinguish the small, albeit unambiguous structural effect of the F8-azo-H8 layer at the air–water interface. This is consistent with the scattering length density profiles in the lower insets. *Via* best fitting, we can derive the scattering length density profile and propose molecular packing model for the interfacial arrangement of F8-azo-H8 molecules in the monolayer. As schematically illustrated in Fig. 7, it is suggested that in the dark, F8-azo-H8 molecules in their *trans* configuration were organized with their long axis perpendicular to the air–water interface (which is consistent with the analysis of isotherms and the findings of Klein *et al.*[39]). In this case, a two-layer model with hydrocarbon and fluorocarbon segments is suggested with a total layer thickness of 4.37 nm and the CF blocks pointing towards the subphase. This model gives the best match in the fitting procedure with the Parratt32 software. Data for other packing and fitting models are provided in the ESI† and resulted in inferior matches between the measurements and fits.

Under UV irradiation, the induced *trans–cis* isomerization gave rise to a random, structureless arrangement. A layer thickness of 0.96 nm was found for a structureless film with random molecular orientation. Assuming a regular orientation in the *cis* configuration with the azobenzene moieties in contact with the water subphase, both the fluorocarbon and hydrocarbon chains pointing towards air did not provide a satisfactory result of the

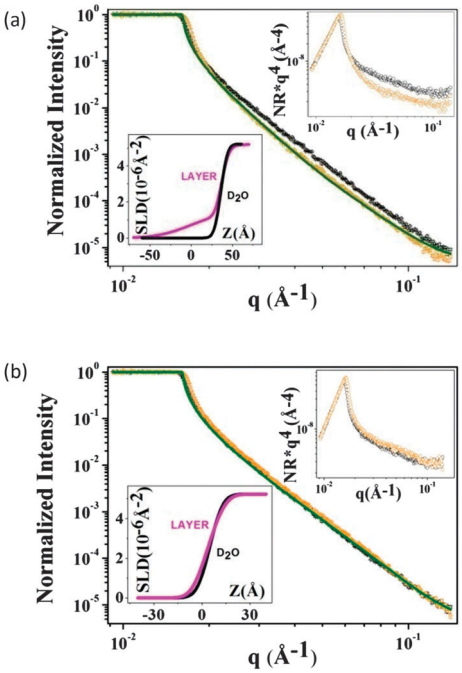

Fig. 6 Neutron reflectivity curves (normalized intensity *vs.* q) of the F8-azo-H8 monolayer on a D_2O subphase. Lower insets: Scattering length density profiles; upper insets: normalized intensity (NR) × q^4 *versus* q. Colour legend: D_2O (black), F8-azo-H8 layer (orange) and fit (green). (a) Dark experiment (surface pressure = 2 mN m^{-1}). (b) Under UV irradiation (surface pressure = 12 mN m^{-1}).

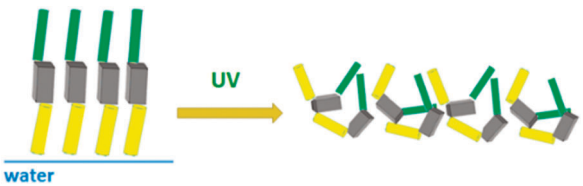

Fig. 7 Proposed model of F8-azo-H8 monolayer at the water–air interface before and after exposure to UV light.

fit (see ESI†). This configuration-induced change in the packing order was accompanied by a decrease in interfacial viscoelastic moduli and a concurrent increase in surface pressure, as documented by the experimental results reported above.

To visualize more details of the layer structure, SFM measurements were made on samples that were transferred from the air–water interface onto solid supports. In samples that were transferred under white-light illumination (*trans* configuration), we observed partial coverage of the Si surface by a thin film (Fig. 8a). A line profile across the steps revealed a film thickness of 4.1 nm (Fig. 8b), which is about 10% thinner than the layer thickness that was derived from the neutron reflectometry results (4.4 nm). We attribute this marginal decrease in film thickness to the effects of drying during the transfer. In samples that were transferred directly after illumination with UV light (*cis* configuration), we observed island structures of up to 160 nm in height and 2 μm in width. In between the island structures, no steps were observed, which indicates full coverage

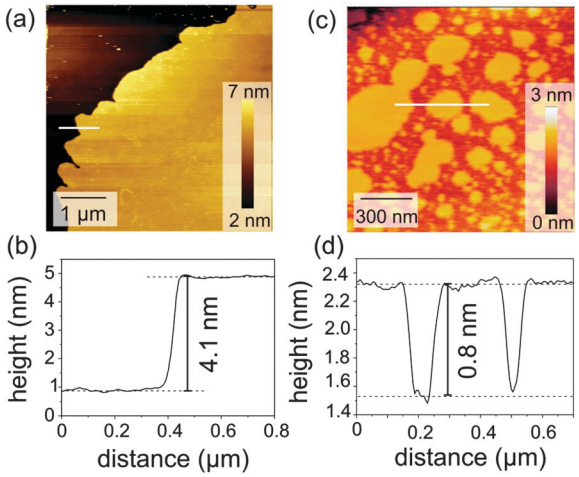

Fig. 8 SFM images of F8-azo-H8 layers transferred onto a Si wafer. (a) Topography of a film in *trans* configuration transferred under white-light illumination at a surface pressure of 2 mN m^{-1}. (b) Line profile at one edge of the film in (a). (c) Topography of a 2 μm wide crystal of a sample that was transferred under UV irradiation (*cis* configuration). (d) Line profile across the island structures of (c).

of the substrate by a monolayer film. However, on top of the islands a patchy structure was observed (Fig. 8c). Height analysis of the patchy structure revealed a thickness of 0.8 nm (Fig. 8d). The latter indicates that UV light can induce a conformational change to *cis*, resulting in a film thickness of <1 nm, which was also concluded by neutron reflectometry.

III.2. Characterisation of the hydrogenated H8-azo-H8 Langmuir layers

The specific molecular structure of F8-azo-H8 is apparently responsible for its observed behaviour and in particular its responsiveness with the resulting tunability of the monolayer by light irradiation. It turns out that the fluorocarbon component of the F8-azo-H8 molecule plays a vital role as it is responsible for the presence of a strong dipole in the F–H direction and therefore, along with the extended and stiff molecular shape of the azobenzene moiety in the *trans* configuration, yields the perpendicular order indicated in Fig. 7. When the azobenzene fragment changes its configuration to *cis* under the influence of UV light, an additional strong dipole is generated by the *cis*-azobenzene moiety, which may destructively interfere with the strong dipole and in combination with the substantial change in molecular shape leads to loss of the specific molecular order. To confirm the particular structure-guiding property of the fluorocarbon chain, we performed experiments under similar conditions with the analogous non-fluorinated azobenzene derivative H8-azo-H8, which contains two identical hydrocarbon chains instead of a fluorocarbon chain. In the *trans* configuration under dark conditions, the H8-azo-H8 molecule did not possess a strong dipole moment and due to its low polarity did not interact strongly with the water subphase. Hence, these molecules had an enhanced tendency to aggregate into 3D structures (preferentially at the barrier wall upon compression), which is reflected in the very small apparent surface area,

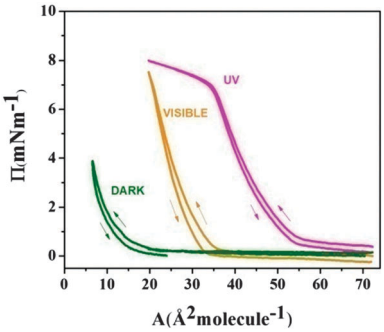

Fig. 9 Surface pressure (*Π*) *versus* molecular area (*A*) isotherms of non-fluorinated H8-azo-H8 monolayers at the air–water interface at 20 °C measured under UV light (right curve in purple, labelled "UV"), under visible light (middle curve in orange, "VISIBLE") and in the dark (left curve in green, "DARK").

visible in the compression–expansion curve of Fig. 9 (green curve labeled "DARK"). Upon UV irradiation, H8-azo-H8 molecules switched to the more polar *cis* form, which led to much stronger attraction to the water subphase. Accordingly, as is visible from the surface pressure–area isotherms, the molecules occupied an area that is about three times larger in the *cis* configuration under UV irradiation compared to the *trans* isomer in the dark (Fig. 9). Under illumination by visible light, the molecular surface requirement lies between the UV and dark conditions, which may be caused by photostationary equilibrium between the *cis* and *trans* configurations with both forms being present simultaneously. In all cases, the compression–expansion cycles show no significant hysteresis (as for F8-azo-H8), which indicates full reversibility of the deformation of the layer during compression on the time scale of the experiment.

The time-resolved change in surface pressure under varying illumination conditions (dark-UV irradiation-dark) is presented in Fig. 10. As in the case of F8-azo-H8 mentioned above (although the values are not as high), a significant increase in pressure was observed when switching on the UV irradiation, which is explained by the substantial increase in the surface requirement of the molecules switching from the *trans* (in the dark) to the *cis* configuration (UV). The curve rapidly reached saturation and

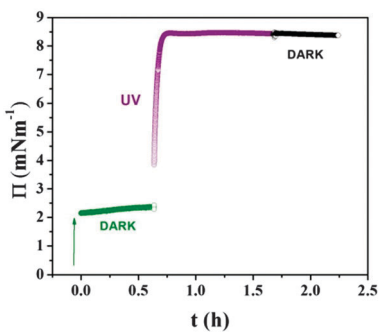

Fig. 10 Surface pressure (*Π*) *versus* time (*t*) of a H8-azo-H8 monolayer at an air–water interface at 20 °C in the dark (left curve in green, labelled "DARK"), under UV irradiation (middle curve in purple, "UV"), and in the dark (right curve segment in black, "DARK").

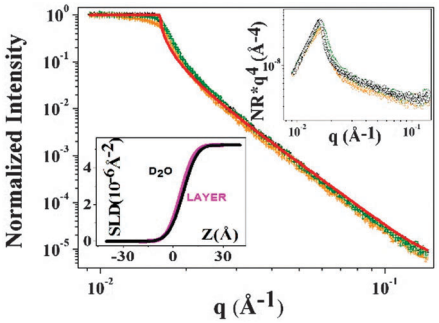

Fig. 11 Neutron reflectivity curve (normalized intensity *vs.* *q*) of the H8-azo-H8 monolayer on a D_2O subphase in the absence of light and under UV irradiation with the scattering length density profile in the lower inset. Upper inset: Normalized intensity (NR) × q^4 *versus* *q*. Colour legend: D_2O (black), H8-azo-H8, dark (orange), H8-azo-H8, UV (green) and fit (red). Surface pressure = 2 mN m^{-1} for dark and 8 mN m^{-1} for UV.

Fig. 12 Proposed model of the H8-azo-H8 monolayer at the air–water interface before and after exposure to UV light.

when the light was switched off after about 1 h of irradiation, the pressure stayed constant (as measured for 0.5 h). The data indicate that the H8-azo-H8 monolayer was stable under these experimental conditions.

Furthermore, the neutron reflectivity results in different representations (as in Fig. 6 above), as shown in Fig. 11, and suggest a different model of the molecular arrangement of H8-azo-H8 (Fig. 12). The molecular packing that provides the best fit to the reflectivity curves indicates a loose random organization of the molecules and a layer thickness of 0.65 nm with no significant effect of light irradiation on the level of organization. Interestingly, the H8-azo-H8 interface exhibited a viscous rheological response that is indistinguishable from the water subphase (data not shown).

IV. Conclusions

We investigated the structural and rheological properties of semifluorinated and fully hydrogenated azobenzene derivatives at the water–air interface under different conditions of light irradiation. Building on earlier studies of related SFA systems, which demonstrated the intriguing ability of these molecules to hierarchically self-assemble at fluid interfaces, we examined here the role of UV light as a specific trigger on the properties and stability of monolayers of SFAB F8-azo-H8 and its non-fluorinated analogue H8-azo-H8. UV irradiation was found to significantly influence the interfacial organization and viscoelasticity of the SFAB derivative F8-azo-H8 with the structure-guiding motif of the fluorinated alkyl chain, whereas it had a significantly weaker effect on the symmetric hydrocarbon derivative H8-azo-H8. Based on the well-known effect of irradiation

by UV and visible light on *cis–trans* isomerization, such exposure to light also markedly influences the packing behaviour of the SFA azobenzene molecules in a reversible way. We conclude that a combination of this effect and the dipole that is associated with the F-chain in F8-azo-H8 provides a transition from well-organized vertically oriented structures to random packing, accompanied by a decrease in viscoelastic moduli and an increase in surface pressure. These findings confirm the reconfigurability of such responsive interfaces and provide the means of tailoring their mechanical properties at will by exploiting the sensitivity of their molecular configuration to UV irradiation. This behavior might be exploited in responsive fluid interfaces for potential applications such as light-triggered 2D actuation layers and photoswitchable lubricating films.

Acknowledgements

Partial support has been received by the Greek General Secretariat for Research and Technology (Heraclitos II program 2011) and the EU (FP7 Infrastructure ESMI GA-262348). This study is based on experiments performed at the AMOR neutron reflectometer at the Swiss Spallation Neutron Source (SINQ), Paul Scherrer Institute, Villigen, Switzerland. Dan Li thanks CSC for support.

References

1 (*a*) A. C. Balazs and J. Aizenberg, Reconfigurable soft matter, *Soft Matter*, 2014, **10**(9), 1244–1245; (*b*) R. Geryak and V. V. Tsukruk, Reconfigurable and actuating structures from soft materials, *Soft Matter*, 2014, **10**(9), 1246–1263.

2 J. Zhang, X. Li and X. Li, Stimuli-triggered structural engineering of synthetic and biological polymeric assemblies, *Prog. Polym. Sci.*, 2012, **37**(8), 1130–1176.

3 (*a*) C. G. Clark, Jr., G. A. Floudas, Y. J. Lee, R. Graf, H. W. Spiess and K. Müllen, Molecularly Tethered Amphiphiles as 3-D Supramolecular Assembly Platforms: Unlocking a Trapped Conformation, *J. Am. Chem. Soc.*, 2009, **131**(24), 8537–8547; (*b*) Y. J. Lee, C. G. Clark, R. Graf, M. Wagner, K. Mullen and H. W. Spiess, Solid-State Organization of Semifluorinated Alkanes Probed by F-19 MAS NMR Spectroscopy, *J. Phys. Chem. B*, 2009, **113**(5), 1360–1366; (*c*) E. Nuñez, C. G. Clark, Jr., W. Cheng, A. Best, G. Floudas, A. N. Semenov, G. Fytas and K. Müllen, Thermodynamic, Structural, and Nanomechanical Properties of a Fluorous Biphasic Material, *J. Phys. Chem. B*, 2008, **112**(21), 6542–6549.

4 (*a*) M. P. Krafft and J. G. Riess, Chemistry, Physical Chemistry, and Uses of Molecular Fluorocarbon-Hydrocarbon Diblocks, Triblocks, and Related Compounds-Unique ''Apolar'' Components for Self-Assembled Colloid and Interface Engineering, *Chem. Rev.*, 2009, **109**(5), 1714–1792; (*b*) G. L. Gaines, Surface-Activity Of Semifluorinated Alkanes – F(CF2)M(CH2)NH, *Langmuir*, 1991, **7**(12), 3054–3056; (*c*) M. P. Krafft and M. Goldmann, Monolayers made from fluorinated amphiphiles, *Curr. Opin. Colloid Interface Sci.*, 2003, **8**(3), 243–250; (*d*) M. Broniatowski and P. Dynarowicz-Latka, Semifluorinated alkanes – primitive surfactants of fascinating properties, *Adv. Colloid Interface Sci.*, 2008, **138**(2), 63–83.

5 B. L. Feringa, R. A. van Delden, N. Koumura and E. M. Geertsema, Chiroptical molecular switches, *Chem. Rev.*, 2000, **100**(5), 1789–1816.

6 G. S. Kumar and D. C. Neckers, Photochemistry of Azobenzene-Containing Polymers, *Chem. Rev.*, 1989, **89**(8), 1915–1925.

7 S. Xie, A. Natansohn and P. Rochon, Recent Developments In Aromatic Azo Polymers Research, *Chem. Mater.*, 1993, **5**(4), 403–411.

8 A. Kocer, M. Walko, W. Meijberg and B. L. Feringa, A light-actuated nanovalve derived from a channel protein, *Science*, 2005, **309**(5735), 755–758.

9 O. V. Yaroshchuk, A. D. Kiselev, Y. Zakrevskyy, T. Bidna, J. Kelly, L. C. Chien and J. Lindau, Photoinduced three-dimensional orientational order in side chain liquid crystalline azopolymers, *Phys. Rev. E: Stat., Nonlinear, Soft Matter Phys.*, 2003, **68**(1), 011803.

10 B. L. Feringa, W. F. Jager and B. Delange, Organic Materials For Reversible Optical-Data Storage, *Tetrahedron*, 1993, **49**(37), 8267–8310.

11 Z. F. Liu, K. Hashimoto and A. Fujishima, Photoelectrochemical Information-Storage Using An Azobenzene Derivative, *Nature*, 1990, **347**(6294), 658–660.

12 T. Ikeda, O. Tsutsumi and Y. L. Wu, Optical switching and image storage by means of photochromic liquid crystals, *Mol. Cryst. Liq. Cryst.*, 2000, **347**, 245–257.

13 W. A. Velema, W. Szymanski and B. L. Feringa, Photopharmacology: Beyond Proof of Principle, *J. Am. Chem. Soc.*, 2014, **136**(6), 2178–2191.

14 T. König, L. M. Goldenberg, O. Kulikovska, L. Kulikovsky, J. Stumpe and S. Santer, Reversible structuring of photosensitive polymer films by surface plasmon near field radiation, *Soft Matter*, 2011, **7**(9), 4174.

15 N. S. Yadavalli, M. Saphiannikova, N. Lomadze, L. M. Goldenberg and S. Santer, Structuring of photosensitive material below diffraction limit using far field irradiation, *Appl. Phys. A: Mater. Sci. Process.*, 2013, **113**(2), 263–272.

16 Y. Zakrevskyy, M. Richter, S. Zakrevska, N. Lomadze, R. von Klitzing and S. Santer, Light-Controlled Reversible Manipulation of Microgel Particle Size Using Azobenzene-Containing Surfactant, *Adv. Funct. Mater.*, 2012, **22**(23), 5000–5009.

17 R. Wustneck, V. B. Fainerman and V. Zauls, Characterization and modeling of *cis–trans* photoisomerization of a trifluoromethoxy-substituted metacrylate copolymer monolayer at a fluid interface, *J. Phys. Chem. B*, 1999, **103**(18), 3587–3592.

18 I. Muzikante, L. Gerca, E. Fonavs, M. Rutkis, D. Gustina, E. Markava, B. Stiller, L. Brehmer and G. Knochenhauer, Self-assembled monolayers of azobenzene functionalized 1,3,5-triazine-4,6-dithiols, *Mater. Sci. Eng., C: Biomimetic Supramol. Syst.*, 2002, **22**(2), 339–343.

19 W. B. Caldwell, D. J. Campbell, K. M. Chen, B. R. Herr, C. A. Mirkin, A. Malik, M. K. Durbin, P. Dutta and K. G. Huang, A Highly Ordered Self-assembled Monolayer Film of an

Azobenzenealkanethiol on Au(111) – Electrochemical Properties and Structural Characterization by Synchrotron In-Plane X-Ray-Diffraction, Atomic-Force Microscopy, and Surface-Enhanced Raman-Spectroscopy, *J. Am. Chem. Soc.*, 1995, **117**(22), 6071–6082.

20 S. D. Evans, S. R. Johnson, H. Ringsdorf, L. M. Williams and H. Wolf, Photoswitching of azobenzene derivatives formed on planar and colloidal gold surfaces, *Langmuir*, 1998, **14**(22), 6436–6440.

21 K. S. Yim and G. G. Fuller, Influence of phase transition and photoisomerization on interfacial rheology, *Phys. Rev. E: Stat., Nonlinear, Soft Matter Phys.*, 2003, **67**(4), 041601.

22 E. Chevallier, A. Mamane, H. A. Stone, C. Tribet, F. Lequeux and C. Monteux, Pumping-out photo-surfactants from an air–water interface using light, *Soft Matter*, 2011, **7**(17), 7866–7874.

23 E. Chevallier, C. Monteux, F. Lequewx and C. Tribet, Photofoams: Remote Control of Foam Destabilization by Exposure to Light Using an Azobenzene Surfactant, *Langmuir*, 2012, **28**(5), 2308–2312.

24 T. G. Shang, K. A. Smith and T. A. Hatton, Photoresponsive surfactants exhibiting unusually large, reversible surface tension changes under varying illumination conditions, *Langmuir*, 2003, **19**(26), 10764–10773.

25 B. A. Cicciarelli, T. A. Hatton and K. A. Smith, Dynamic surface tension behavior in a photoresponsive surfactant system, *Langmuir*, 2007, **23**(9), 4753–4764.

26 B. A. Cicciarelli, J. A. Elia, T. A. Hatton and K. A. Smith, Temperature dependence of aggregation and dynamic surface tension in a photoresponsive surfactant system, *Langmuir*, 2007, **23**(16), 8323–8330.

27 Z. F. Liu, K. Morigaki, T. Enomoto, K. Hashimoto and A. Fujishima, Kinetic-Studies on the Thermal *CisTrans* Isomerization of an Azo Compound in the Assembled Monolayer Film, *J. Phys. Chem.*, 1992, **96**(4), 1875–1880.

28 I. Mita, K. Horie and K. Hirao, Photochemistry In Polymer Solids. 9. Photoisomerization of azobenzene in a polycarbonate film, *Macromolecules*, 1989, **22**(2), 558–563.

29 B. Kumar and K. A. Suresh, Kinetics of *trans–cis* isomerization in azobenzene dimers at an air–water interface, *Phys. Rev. E: Stat., Nonlinear, Soft Matter Phys.*, 2009, **80**(2), 021601.

30 T. Seki, M. Sakuragi, Y. Kawanishi, Y. Suzuki, T. Tamaki, R. Fukuda and K. Ichimura, Command Surfaces of Langmuir–Blodgett-Films – Photoregulations of Liquid-Crystal Alignment by Molecularly Tailored Surface Azobenzene Layers, *Langmuir*, 1993, **9**(1), 211–218.

31 (*a*) B.-C. Yu, Y. Shirai and J. M. Tour, Syntheses of new functionalized azobenzenes for potential molecular electronic devices, *Tetrahedron*, 2006, **62**(44), 10303–10310; (*b*) J. Lux and J. Rebek, Jr., Reversible switching between self-assembled homomeric and hybrid capsules, *Chem. Commun.*, 2013, **49**(21), 2127–2129; (*c*) R. Stangenberg, *Oberflächenstrukturierte amphiphile Polyphenylendendrimere zur Imitation natürlicher Transportproteine*, PhD thesis, Fachbereich Chemie, Pharmazie und Geowissenschaften der Johannes Gutenberg-Universität Mainz, Germany, 2013.

32 R. Stangenberg, C. Grigoriadis, H.-J. Butt, K. Muellen and G. Floudas, Switchable dielectric permittivity with temperature and Dc-bias in a semifluorinated azobenzene derivative, *Colloid Polym. Sci.*, 2014, **292**(8), 1939–1948.

33 C. F. Brooks, G. G. Fuller, C. W. Frank and C. R. Robertson, An interfacial stress rheometer to study rheological transitions in monolayers at the air–water interface, *Langmuir*, 1999, **15**(7), 2450–2459.

34 D. Clemens, P. Gross, P. Keller, N. Schlumpf and M. Konnecke, AMOR – the versatile reflectometer at SINQ, *Physica B*, 2000, **276**, 140–141.

35 M. Gupta, T. Gutberlet, J. Stahn, P. Keller and D. Clemens, AMOR – the time-of-flight neutron reflectometer at SINQ/PSI, *Pramana*, 2004, **63**(1), 57–63.

36 L. G. Parratt, Surface Studies Of Solids By Total Reflection Of X-Rays, *Phys. Rev.*, 1954, **95**(2), 359–369.

37 http://www.ncnr.nist.gov/resources/sldcalc.html, N. I. o. S. a. T. C. f. N. R. S. L. D. C.

38 (*a*) I. Jasiuk, J. Chen and M. F. Thorpe, Elastic Moduli of Two Dimensional Materials with Polygonal and Elliptical Holes, *Appl. Mech. Rev.*, 1994, **47**(1S), S18–S28; (*b*) A. Bhaskar, The effective Poisson ratio of random cellular matter having bending dominated architecture, *Europhys. Lett.*, 2009, **87**, 18004; (*c*) K. V. Tretiakov and K. W. Wojciechowski, Poisson's ratio of simple planar 'isotropic' solids in two dimensions, *Phys. Status Solidi B*, 2007, **244**(3), 1038–1046.

39 C. O. Klein, L. de Viguerie, C. Christopoulou, U. Jonas, C. G. Clark, Jr., K. Muellen and D. Vlassopoulos, Viscoelasticity of semifluorinated alkanes at the air/water interface, *Soft Matter*, 2011, **7**(17), 7737–7746.

